



Recent changes of the dissolved oxygen distribution in the deep convection cell of the southern Adriatic Sea

R. Martellucci^{a,*}, M. Menna^a, E. Mauri^a, A. Pirro^a, R. Gerin^a, F. Paladini de Mendoza^b, R. Garić^c, M. Batistić^c, V. di Biagio^a, P. Giordano^d, L. Langone^d, S. Miserocchi^d, A. Gallo^a, G. Notarstefano^a, G. Savonitto^a, A. Bussani^a, M. Pacciaroni^a, P. Zuppelli^a, P.-M. Poulain^e

^a National Institute of Oceanography and Applied Geophysics (OGS), Borgo Grotta Gigante 42/c, 34010 Trieste, Italy

^b CNR-ISMAR, Arsenal e Castello, 2737/F, 30122 Venice, VE, Italy

^c Institute for Marine and Coastal Research, University of Dubrovnik, Kneza Damjana Jude 12, 20000 Dubrovnik, Croatia

^d CNR-ISP, Via P. Gobetti, 101, 40129 Bologna, BO, Italy

^e Centre for Maritime Research and Experimentation (CMRE), La Spezia 19126, Italy

ARTICLE INFO

Keywords:

Dissolved oxygen
South Adriatic Sea
BiOS
Ocean dynamics
Dense water formation

ABSTRACT

The dynamics of dissolved oxygen in the ocean are of crucial importance for understanding marine ecosystems, with influences ranging from exchange with the atmosphere to biological processes and ocean circulation. In this study, we focus on the southern Adriatic Sea, an essential component of the Eastern Mediterranean “conveyor belt”, to investigate long-term oxygen dynamics and its driving factors. We use cross-platform datasets from 2013 to 2020, including remote sensing data, model reanalysis and in-situ observations from Argo floats, ocean gliders and ship-based measurements. Our analysis investigate the interplay of physical, biological and atmospheric forcing that drive oxygen variability. The distribution of dissolved oxygen in the southern Adriatic Sea is influenced by vertical mixing, advection of water masses and ecosystem dynamics. In the surface layer, the variability of dissolved oxygen is triggered by annual primary production and deep convection events. The dynamics in the intermediate and the deep layers are instead primarily influenced by physical processes, such as the vertical mixing and the water masses inflow from the adjacent sub-basins, which is driven by the periodic reversals of northern Ionian Gyre circulation. In particular our study reveals that the water masses advective dynamics driving the increase and decrease of dissolved oxygen have drastically changed in recent years. The highest dissolved oxygen concentrations are currently observed during the northern Ionian Gyre anticyclonic phase, while they have been previously documented during the cyclonic phase. This change appears to be connected with the significant increase in salinity observed in the southern Adriatic Sea in the same period and contributes to a better understanding of the processes that determine oxygen distribution in the Eastern Mediterranean basin.

1. Introduction

The distribution of dissolved oxygen in the ocean is significantly influenced by exchanges with the atmosphere, ocean circulation, and biological processes (Falkowski et al., 2011; Pierce et al., 2012) and plays a central role in our knowledge of marine ecosystems (Gilly et al., 2013; Breitburg et al., 2018). The increase or decrease in oxygen concentration (Garcia and Keeling, 2001) depends on the balance between biological production and consumption (i.e., community respiration) and physical inputs of oxygen-poor or oxygen-rich waters (e.g.,

dissolved oxygen produced by phytoplankton during spring blooms). Oxygen depletion has been observed in the global ocean in recent years, and climate models predict further declines in the future (Matear et al., 2000; Oschlies et al., 2018; Stramma et al., 2010; Reale et al., 2021). The main reason for this condition can be attributed to the increase in global temperature, which leads to a decrease in oxygen solubility and deep water ventilation (i.e., increase in stratification and weakening of ocean overturning circulation), as well as an increase in oxygen consumption (Breitburg et al., 2018; Oschlies et al., 2018).

In the context of global ocean deoxygenation (Schmidtke et al.,

* Corresponding author.

E-mail address: rmartellucci@ogs.it (R. Martellucci).

<https://doi.org/10.1016/j.jmarsys.2024.103988>

Received 13 May 2023; Received in revised form 9 May 2024; Accepted 12 May 2024

Available online 13 May 2024

0924-7963/© 2024 The Authors. Published by Elsevier B.V. This is an open access article under the CC BY license (<http://creativecommons.org/licenses/by/4.0/>).

2017), oxygen dynamics are of particular interest in areas where oceanic processes connect surface and deep layers (Marshall and Schott, 1999). In these areas, the sinking of surface waters brings oxygen into the deep ocean layers, benefiting deep ocean ecosystems (Keeling et al., 2010). In the Mediterranean Sea, deep water formation and associated convection phenomena occur in three sites: the Gulf of Lion (northwestern Mediterranean Sea; Schott et al., 1996, Houpert et al., 2016, Macias et al., 2018, Testor et al., 2018), the Cretan Sea (Malanotte-Rizzoli et al., 1997), and the southern Adriatic Sea (Gačić et al., 2002; Pirro et al., 2022).

The oxygen cycle and budget over the northwestern Mediterranean Sea and the Cretan Sea deep convection areas have been examined and updated in literature (Souvermezoglou et al., 1999; Coppola et al., 2018; Ulses et al., 2021), while similar analyses are rather fragmentary for the southern Adriatic (Manca et al., 2002, 2004, 2006; Lipizer et al., 2014; Mavropoulou et al., 2020). Although thermohaline variability in the South Adriatic Pit (SAP) has been extensively studied in recent decades, long-term oxygen dynamics have never been studied in detail.

In the southern Adriatic Sea (Fig. 1a), convection phenomena occurred during winter season, triggered by episodes of cold and dry northeasterly winds (e.g., Bora) that create favourable conditions for deep convection and the resulting formation of Adriatic Dense Water (AdDW) (Manca et al., 2002; Gačić et al., 2002; Pirro et al., 2022). These cold and dry winds play a central role also in the production of the North Adriatic Dense Water (NAdDW) (Mihanovic et al., 2013; Chiggiato et al., 2016; Mauri et al., 2016; Querin et al., 2016; Paladini de Mendoza et al., 2023), which occasionally flows into the SAP after winter cooling, ventilating the deepest layers of the SAP (NAdDW: potential density anomaly $>29.2 \text{ kg m}^{-3}$, Temperature = $11.35 \text{ }^\circ\text{C} \pm 1.408$, Salinity = 38.3 ± 0.28 ; Artegiani et al., 1997, Bensi et al., 2013). Moreover, oceanographic and biogeochemical features in the SAP are strongly influenced by the advection of different water masses from the Ionian Sea (Manca et al., 2006, Civitarese et al., 2010, Menna et al., 2022a, 2022b), which enter the SAP through the Strait of Otranto (Fig. 1a). The advection of large amount of water masses together with deep water formation events produces a very short (~26 months) renewal time of

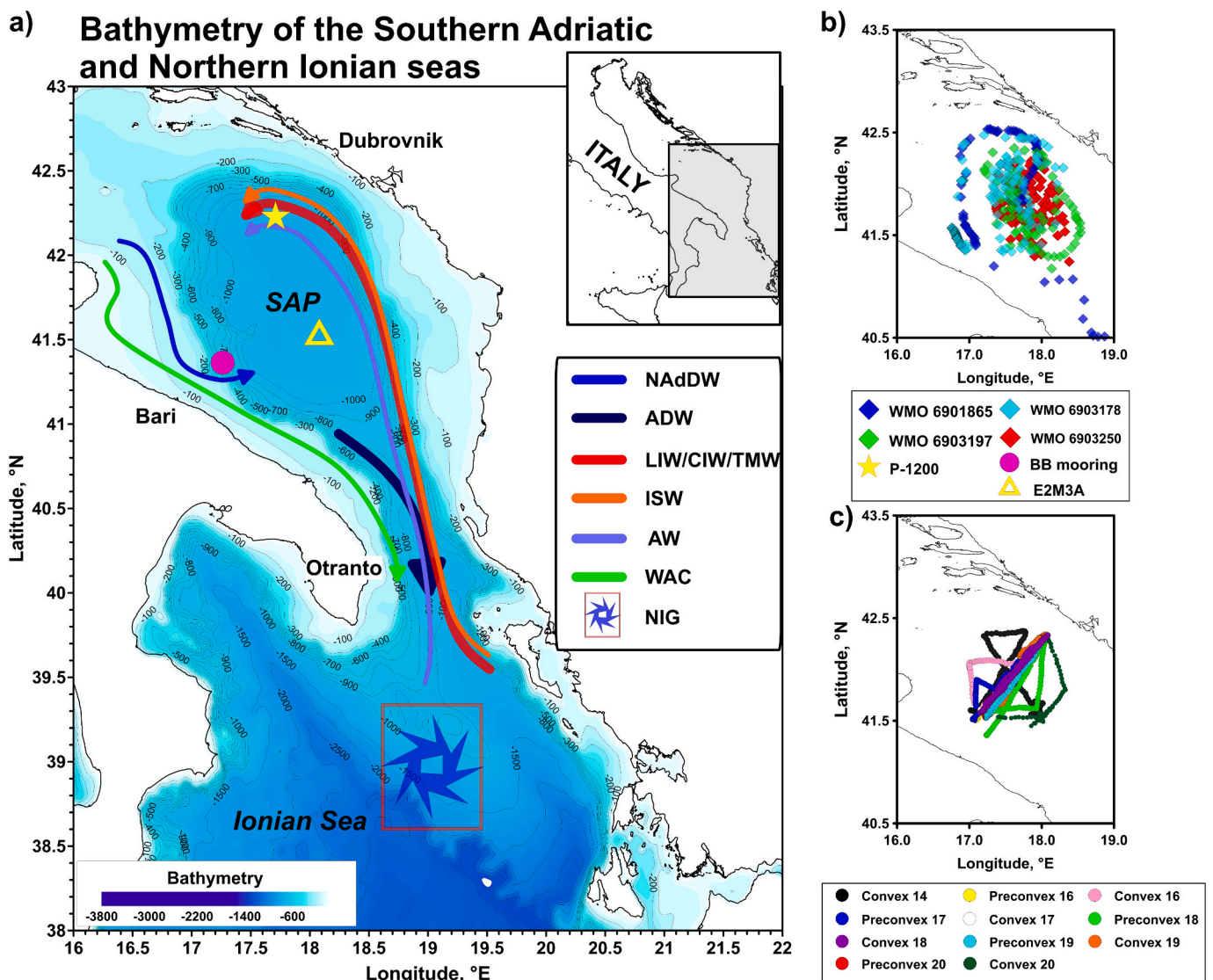


Fig. 1. Bathymetry of the southern Adriatic Pit (SAP) and northern Ionian Sea, with schematic representation of the main water masses (NAdDW: North Adriatic dense water, AdDW: Adriatic dense water, LIW: Levantine intermediate water, CIW: Cretan intermediate water, ISW: Ionian surface water, AW: Atlantic water, WAC: western Adriatic current, from Manca et al. (2006), NIG: Northern Ionian Gyre, from Gačić et al. (2021) and fixed stations (BB mooring, magenta circle, located in the Bari Canyon, E2M3A, yellow triangle and P-1200 L-Term station, yellow star). Geographical positions (b) of the Argo float profiles (6,901,865 blue diamond, 6,903,178 cyan diamond, 6,903,197 green diamond and 6,903,250 red diamond); Glider surfacing positions during the missions listed in the legend (c). (For interpretation of the references to colour in this figure legend, the reader is referred to the web version of this article.)

the water in the SAP (Vilibić and Orlić, 2002).

The Strait of Otranto has a maximum depth of about 800 m (Yari et al., 2012), therefore the vertical distribution of water masses in the northern Ionian Sea plays a key role in the inflow of different water masses into the southern Adriatic. Specifically, the surface layer (0–150 m) in the northern Ionian Sea is characterized by Atlantic water (AW) and Ionian surface water (ISW), while the intermediate layer (150–1000 m) is characterized by Cretan Intermediate Water (CIW), Levantine Intermediate Water (LIW) and Transitional Mediterranean Water (TMW) (Manca et al., 2003). The latter represents the Oxygen Minimum Layer (OML) ($\sim 185 \mu\text{mol kg}^{-1}$) in the Ionian Sea (Manca et al., 2003; Manca et al., 2006), while the CIW has the highest oxygen content ($\sim 205 \mu\text{mol kg}^{-1}$) in the Northern Ionian Sea, Manca et al., 2003) in the intermediate layer of the northern Ionian Sea. Compared to the western Mediterranean Sea (Coppola et al., 2018), the LIW ($\sim 195 \mu\text{mol kg}^{-1}$) in the northern Ionian Sea has a higher oxygen content because it has been formed recently (Manca et al., 2003).

The inflow through the Strait of Otranto depends on the change of circulation in the northern Ionian Sea from cyclonic to anticyclonic (Civitarese et al., 2010; Gačić et al., 2010; Menna et al., 2019; Batistić et al., 2019). The most widely recognised and cited process to explain such quasi-decadal reversal is a feedback mechanism called the Adriatic-Ionian Bimodal Oscillation System (BiOS, Gačić et al., 2010; Civitarese et al., 2010, Civitarese et al., 2023) and is driven by the difference in salinity between the salty and warmer waters originating from the eastern Mediterranean Sea and the less saline water of Atlantic origin flowing from the Sicily Channel (Gačić et al., 2011, 2014, 2021; Menna et al., 2019; Menna et al., 2022a, 2022b). The cyclonic phase of NIG results in enhanced advection of surface ISW and LIW/CIW into the Adriatic, while the anticyclonic phase involves advection of less saline AW and TMW (Civitarese et al., 2010). The alternation of cyclonic and anticyclonic phases affects the depth of the OML (i.e., TMW depth) in the Ionian Sea and the associated inflow to the SAP. During the 1995 cyclonic phase it reached greater depths (1000–1200 m), while during the 1999 anticyclonic phase, the OML (500–800 m) was shallower due to the doming of the NIG (Manca et al., 2003). This shift triggered by the BiOS mechanism also affects the other biochemical properties of the SAP (Civitarese et al., 2010; Krokos et al., 2014; Mavropoulou et al., 2020). Civitarese et al. (2010) showed that nutrient concentrations are highest during the anticyclonic phase, due to the presence of a shallow pycnocline in the northern Ionian Sea, which increases nutrient concentrations and associated primary production (Kovač et al., 2018) and causes further oxygenation in the Subsurface Oxygen Maximum (SOM, Shulenberger and Reid, 1981). Nevertheless, dissolved oxygen measurements in the southern Adriatic are crucial in understanding the ventilation processes in the central and eastern Mediterranean Sea, as the dense water masses formed in the Pit play an important role in driving the deep thermohaline cell of the eastern Mediterranean Sea “conveyor belt” (Bignami et al., 1990; Malanotte-Rizzoli and Eremeev, 1999; Manca et al., 2002).

This work focuses on the long-term oxygen dynamics and the drivers of oxygenation and depletion by integrating different data sets to improve the knowledge of deep oxygenation processes in a key area of the eastern Mediterranean Sea. The southern Adriatic Sea is a natural laboratory to study in depth the ocean processes. For a decade, oceanographic cruises, moorings and autonomous instruments (floats and gliders) have been providing physical and biogeochemical observations in this area (Pranić et al., 2021), representing one of the longest continuous observatories in the Mediterranean Sea.

The paper is organized as follows: Section 2 describes the multiplatform datasets and the data analysis. Section 3 shows the results concerning dissolved oxygen dynamics and the relation with the external forcing. A discussion is provided in Section 4, and concluding remarks are given in Section 5.

2. Data and methods

The datasets used for this study are retrieved from in-situ data, satellite products, and model reanalysis in the period 2013–2020. The E2M3A observatory, composed of a surface buoy and a deep mooring active since 2006 (Cardin et al., 2020) (Fig. 1a), together with the two moorings BB and FF active since 2010, became part of the European Multidisciplinary Sea floor and water column Observatory European Research Infrastructure Consortium in 2021 as South Adriatic regional facility (EMSO-ERIC, De Santis et al., 2022). Several oceanographic cruises (Fig. 1a) performed in L-Term station (p-1200, Batistić et al., 2019), and OGS oceanographic surveys (Santić et al., 2019), have been performed in the area in the same period. In addition, the Argo program (Argo GDAC, Wong et al., 2020) and ocean gliders has improved observational performance in the area (Fig. 1a and b).

They are briefly described hereafter.

- In situ data:
 - twelve Argo floats (temperature and salinity) (Wong et al., 2020, Gallo and Martellucci, 2022, doi:10.13120/BXF7-PB83), four of which were equipped with the oxygen sensor (colored diamonds in Fig. 1b);
 - eleven glider missions (mainly along the transect Bari-Dubrovnik, colored dots in Fig. 1c) (Kokkini et al., 2019; Pirro et al., 2022);
 - monthly shipborne oxygen profile at p-1200 (Batistić et al., 2019) (yellow star in Fig. 1a; 42.22°N, 17.71°E, 1200 m deep), collected between 2016 and 2019. The DO sensors used was SBE43 and DO data were post calibrated after missions;
 - four oceanographic surveys (performing Winkler analysis on in-situ samples);
 - deep mooring BB (magenta circle in Fig. 1a), located in the southern Adriatic at Bari Canyon (approximately at 600 m depth) representing a proxy for dense water cascading produced in the northern Adriatic (Querín et al., 2013; Chiggiato et al., 2016) and at present is part of the “Shelf-slope Observatory Site” of the EMSO regional facility for the South Adriatic Sea. The mooring is positioned at 600 m depth in the main branch of the Bari Canyon and it is composed by several sensors distributed along 100 m mooring line at different depths. Starting from the bottom there is a CTD (SBE 16 v2) positioned 10 m above the water column, a temperature sensor at 20 m and ADCP looking downward at 100 m above the seabed (details on Paladini de Mendoza et al., 2022, Miserochi et al., 2023), the oxygen sensor is a SBE 63;
 - E2M3A, is the “South Adriatic Pit observatory” of EMSO regional facility located in open sea at the centre of the southern Adriatic pit and composed by surface buoy and mooring. The surface buoy is instrumented with meteorological station and radiometers to collect air-sea interaction measurements, sensors for physical (temperature and salinity) and biochemical (oxygen, partial CO₂ and pH) parameters distributed in the mixed layer. The mooring line positioned at the bottom of the South Adriatic Pit houses an instrumental chain with sensors at different depths for physical and chemical measurements from the sea floor (1200 m) to the intermediate layer (150 m), at different depths as explained in detail by Cardin et al., 2020.

The dataset of the EMSO Regional Facility for the south Adriatic Sea is freely accessible at the ERDDAP data server at <https://erddap.emso.eu/erddap/index.html>.

- Satellite data:
 - Daily (1/8° Mercator projection grid) Absolute Dynamic Topography (ADT) derived from altimeter and distributed by Copernicus Marine Environment Monitoring Service (product user manual CMEMS-SL-QUID_008-032-051). The ADT was obtained by the sum of the sea level anomaly and a 20-years synthetic mean estimated by Rio et al., 2014 over the 1993–2012 period.

- Daily surface chlorophyll-a field derived from products of ocean colour satellite observations (DOI:10.48670/moi-00300 OCEANCOLOUR_MED_BGC_L4_MY_009_144 (Volpe et al., 2019) distributed by Copernicus Marine Service.
- Model products:
 - Monthly surface salinity, temperature and current fields derived from the Mediterranean Sea physics reanalysis product distributed by Copernicus Marine Service, Escudier et al., 2021 (DOI:10.25423/CMCC/MEDSEA_MULTYEAR_PHY_006_004_E3R1).
 - Daily surface heat fluxes data were extracted in the southern areas of the Adriatic sea from the Copernicus Climate ERA5 hourly data on single levels from 1979 to present dataset (Copernicus climate data store, DOI: 10.24381/cds.adbb2d47).

The oxygen data of autonomous platforms showed values that suggested the need to apply a correction to the data. We are aware of the correction method indicated in the ARGO SOP states (Bittig et al., 2018, Thierry et al., 2022); unfortunately, Takeshita's method (Takeshita et al., 2013) is difficult to apply as the climatology of the area is not well determined due to the very high variability. Other correction techniques as the in-air calibration (Johnson et al., 2015, Bittig et al., 2018, Thierry et al., 2022) are not always possible, in fact except for one recent float, the other ones were of the old type with the sensor not exposed to the air when the float reached the surface. In the case of the gliders the in-air correction cannot be applied. To obtain a robust and consistent oxygen dataset (Gerin et al., 2020a, 2020b, Appendix A), all oxygen data collected with floats and gliders were validated using the results of Winkler samples (Carpenter, 1965) whenever available or using in-situ validated DO data, collected nearby. We performed a direct comparison between Winkler samples and dissolved oxygen profiles, and between different dissolved oxygen profiles (i.e., previously calibrated profiles) using least squares minimization to estimate the offset (Appendix A).

The shapes of the various dissolved oxygen profiles were quite similar differing only by an offset (from $11 \mu\text{mol l}^{-1}$ to $20 \mu\text{mol l}^{-1}$ for Argo floats and from $20 \mu\text{mol l}^{-1}$ to $50 \mu\text{mol l}^{-1}$ for gliders), and the minimization method yielded a very high coefficient of determination, ranging from 0.85 to 0.95 for floats and near 0.82 for gliders (Gerin et al., 2020a, 2020b). Quality-controlled vertical profiles (Wong et al., 2003, Owens and Wong, 2009, Cabanes et al., 2016, 2021) of temperature and salinity derived from Argo floats were used to calculate the time series at different depths (Gallo and Martellucci, 2022; Fig. 2a, b, and c), and mixed layer using the method described in de Boyer Montégut et al. (2004) (i.e., using $0.2 \text{ }^\circ\text{C}$ and 0.03 kgm^{-3} as thresholds). The threshold used to compute the MLD were commonly used for the Adriatic Sea (Kokkini et al., 2019).

To understand the drivers of oxygen variability, the use of products from numerical models was chosen. The consistency of the different data sets (i.e. in situ observations and numerical models) was investigated by comparing the temperature and salinity products of the numerical model and the Argo float data (Appendix A). In particular, the EOFs of the different data sets were calculated as described in Martellucci et al. (2021). The results of the comparison showed high correlation for both spatial and temporal patterns of variability (Fig. B1), thus justifying the use of numerical models to understand the drivers of dissolved oxygen variability.

Monthly means of the Absolute Geostrophic Velocities were used to estimate relative vorticity, which was spatially averaged in the northern Ionian Sea region ($37\text{--}39^\circ\text{N}$ and $17\text{--}19.5^\circ\text{E}$; Notarstefano et al., 2019; Fig. 4). The weekly surface chlorophyll-a field was computed from the daily surface chlorophyll-a dataset.

Reanalysis products (i.e., salinity, sea temperature, and currents) were used to calculate the volume transport through the Strait of Otranto, using the method of Yari et al. (2012). Subsequently, to better understand the phenomenon, it was decided to divide the Strait into a surface and a deep section. This decision was motivated by the

observation reported in the literature (Yari et al., 2012) that the outflow is generally between 400 m and 800 m deep, while the inflow ranges from the surface to 400 m deep.

3. Results

Argo float-derived temperature and salinity profiles were used to determine the interannual variability of thermohaline properties in SAP during 2014–2020 (Fig. 2). In the upper layer (0–150 m, Fig. 2a), summer stratification (indicated by higher temperature and salinity values in July–October) and winter mixing (lower temperature and salinity values in January–March) alternated from year to year, with salinity showing a positive trend. The higher salinities of the whole water column were found in this surface layer (Fig. 2a), with higher values in 2019 and 2020, which is related to the inflow of high saline water of Levantine origin into the SAP (Mihanović et al., 2021; Menna et al., 2022a, 2022b).

In the intermediate layer (150–350 m), the highest temperatures ($14.8\text{--}14.9 \text{ }^\circ\text{C}$) were observed in 2014, 2018, and 2020, and lowest salinity values ($S = 38.75\text{--}38.8$; Fig. 2b) were observed between 2015 and 2016, which were related to the inflow of cooler and less saline water from the northern Adriatic Sea (Kokkini et al., 2019; Mihanović et al., 2021).

In these years the NAddW was relatively lighter than usual, as observed in the Bari canyon ($\leq 29.15 \text{ kg m}^{-3}$; Fig. 2d) and filled the intermediate layer of SAP (Fig. 2b). Positive trends in salinity and temperature were observed between 2017 and 2019 (Fig. 2b).

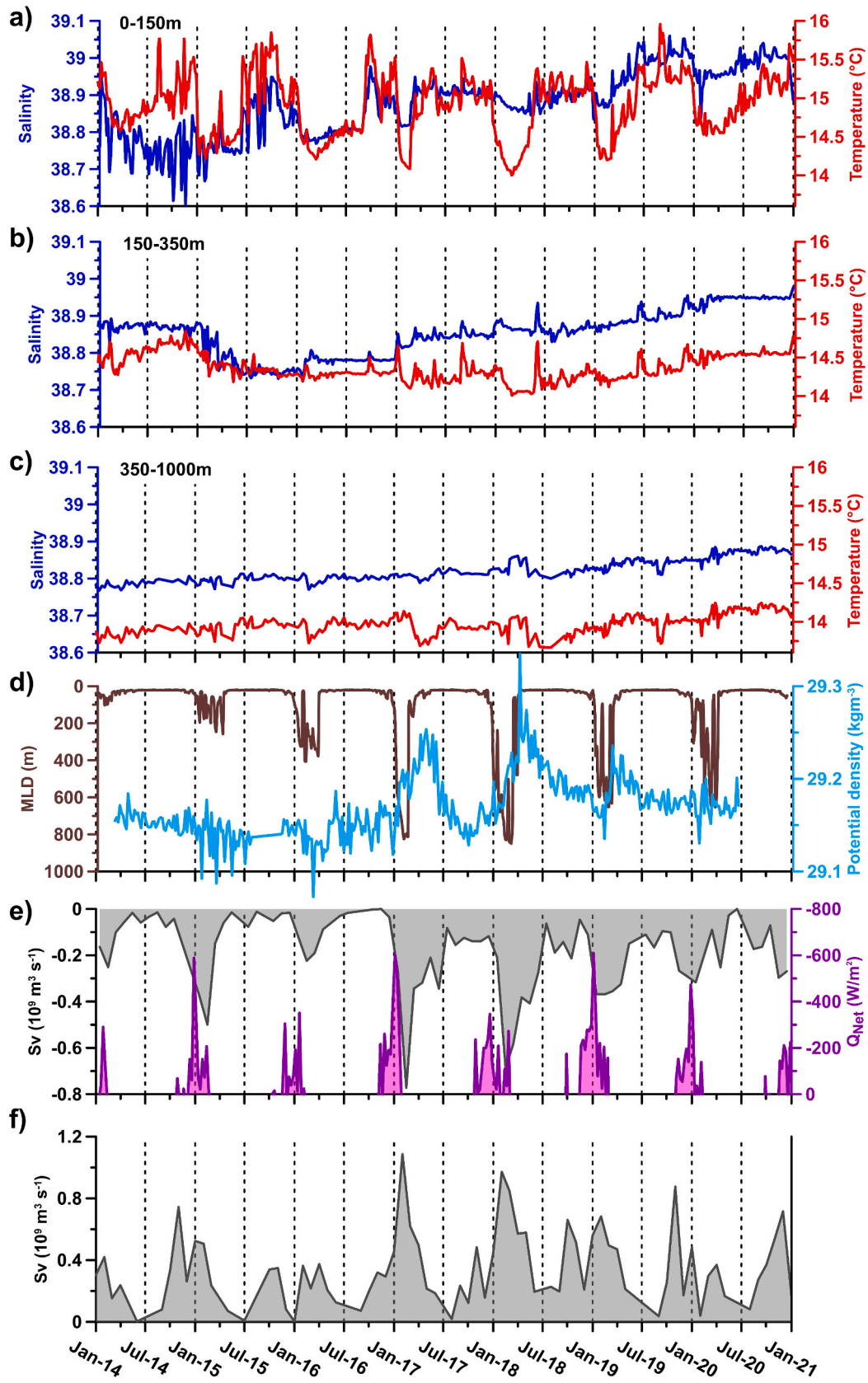
The deep layer (350–1000 m) showed progressive warming ($\sim 0.4 \text{ }^\circ\text{C}$) and salinization (~ 0.1) over time. Convection events in this layer were generally followed by a net decrease in temperature and salinity in the spring (Fig. 2c) due to advection in this season of the NAddW. The signature of this inflow in the interior of SAP was described by density values exceeding 29.2 kg m^{-3} in the Bari canyon time series (Fig. 2d).

The interannual cycle of surface net heat fluxes (Fig. 2e) triggered the mixed layer depth (MLD) in the SAP (Fig. 2d). Weaker winter convection events occurred from 2014 to 2016, when the Q_{net} was weaker and MLD reached ~ 400 m. The highest values (i.e. negative) of surface net heat fluxes occurred during the winter 2017 ($Q_{\text{net}} \sim -600 \text{ W m}^{-2}$), producing a deepening of the MLD nearly to 800 m (Fig. 2d). During 2017, 2018 and 2019 negative heat fluxes persist for a longer period of time concurrently with deep MLD.

The AddW formed during convection events in the SAP outflowed through the Strait of Otranto (Fig. 2e), reaching the highest discharge in February 2017 and 2018 ($\sim 0.7 \text{ Sv}$). Concurrently with the outflow, large amount of water entered in to the SAP (Fig. 2f), the highest inflow occurred during the convection period, reaching the highest values between 2017 and 2018 ($\sim 1.1 \text{ Sv}$).

In the upper layer, coinciding with the photic zone, the variability of dissolved oxygen was mainly influenced by vertical mixing (MLD in Fig. 2d) and biological production (Fig. 3a). During winter convection (i.e., February–April), the concentration of dissolved oxygen had homogeneous values of $\sim 240 \mu\text{mol kg}^{-1}$, while during stratification (i.e., May–November), the layer between 25 m and 70 m depth was characterized by the SOM, with a concentration of dissolved oxygen $> 250 \mu\text{mol kg}^{-1}$ (Fig. 3b). The oxygen content in the SOM layer remained constant between the late spring and early autumn and decreased slowly until the next winter mixing. Years 2018 and 2019 showed the highest oxygen concentrations ($> 250 \mu\text{mol kg}^{-1}$) and temporal persistence, concurrently with higher chlorophyll-a concentrations (Fig. 3a).

Below the SOM, the dissolved oxygen concentration is lower than $210 \mu\text{mol kg}^{-1}$ during the stratified periods, with the exception of 2016 when the dissolved oxygen concentration had the highest values ($\sim 225 \mu\text{mol kg}^{-1}$). This due to the inflow of oxygenated and less saline water NAddW ($S = \sim 38.8$; Fig. 2b), which intruded into the SAP filling the layers from the SOM down to 500 m (Fig. 3c).



(caption on next page)

Fig. 2. Time series of daily temperature (red line) and salinity (blue line) obtained from Argo float dataset spatially averaged in the SAP (Gallo and Martellucci, 2022) between 0 and 150 m (a), 150–350 m (b) and 350–1000 m (c). Daily mixed layer depth (brown line) and daily averaged potential density at 600 m depth (cyan line) in the Bari canyon (d). Average monthly mass transport (black filled line) through the Otranto Strait between 400 and 800 m and weekly surface net heat fluxes (magenta filled line) over the SAP (41.6–42.5°N; 17–18°E) (e). Negative values in (e) refer to outflow from the Strait of Otranto, for Qnet, only negative values are shown. Average monthly mass transport (black filled line) through the Otranto Strait between surface and 400 m (f). (For interpretation of the references to colour in this figure legend, the reader is referred to the web version of this article.)

In the intermediate and deep layers (from 150 m to 1000 m), the distribution of dissolved oxygen is related to the deepening of the MLD during winter convection (Figs. 2d and 3c) and to the inflow and outflow of different water masses during the stratification period. In 2014, the lowest oxygen concentration ($<210 \mu\text{mol kg}^{-1}$) was observed between 100 m and 400 m depth, while the highest oxygen concentration was below 400 m ($\sim 220 \mu\text{mol kg}^{-1}$). In 2015 and 2016, the concentration of dissolved oxygen in the water column was characterized by an alternation of minima (50–100 m and 500–800 m) and maxima (150–350 m and 800–1000 m), which were related to higher and lower values of salinity, respectively. Convection in 2016 mixed the water column to depths of 500 m, resulting in an increase in the concentration of dissolved oxygen in this layer.

The winters of 2017 and 2018 were characterized by deep convection (MLD reached 800 m; Fig. 2d) which mixed the water column down to 800 m depth. The strong convection in these years were mainly due to high heat losses (strong East Atlantic pattern, EA = -1.15 for January 2017 and -1.38 for February 2018; Josey et al., 2011, Reale et al., 2020). The 2017 convection event resulted in deep mixing that drastically changed the water column structure, erasing the double salinity peak shaped between 2015 and 2016 (Fig. 3a and c). After the convection, a sharp decrease in oxygen concentration occurred in the deeper layer (800–1000 m), in connection with the AdDW outflow through the Strait of Otranto (Fig. 2e). This outflow typically occurs between 400 m and the seafloor. In spring (i.e., from March to June), advection of NAdDW brought oxygenated water (dissolved oxygen $> \sim 220 \mu\text{mol kg}^{-1}$) to the 500–1000 m layer, outflowing through from the Bari canyon (Fig. 2d), increasing oxygen levels in the SAP (Fig. 3c). Beginning in late 2019, there was a progressive decrease in dissolved oxygen concentrations between 300 m and 1000 m ($\sim 210 \mu\text{mol kg}^{-1}$) along with an increase in salinity. This was related to the mixing of less oxygenated waters of Levantine origin flowing in to the SAP trough Strait of Otranto (Fig. 2f).

The temporal evolution of dissolved oxygen concentration, averaged over the intermediate and deep layers (150–1000 m depth), show an out of phase behaviour with respect to the NIG vorticity (Fig. 4). Higher oxygen concentrations ($\sim 230 \mu\text{mol kg}^{-1}$) were observed during the NIG anticyclonic phases, characterized by negative vorticity (2012–2013, 2017–2018), and lower concentrations ($\sim 210 \mu\text{mol kg}^{-1}$) during the NIG cyclonic phases, characterized by positive vorticity (2014–2016; 2019–2020). The stronger oxygen increase was observed in 2017, just after the NIG reversal from cyclonic to anticyclonic.

4. Discussion

The interannual variability of dissolved oxygen concentration in the SAP is related to internal and external factors acting in the different ocean layers and influencing each other. Primary production affects dissolved oxygen variability in the surface layer; advection of water masses from adjacent sub-basins affects mainly the intermediate and deep layers; local mixing and convection processes affect the water column in winter with a large interannual variability (Kokkini et al., 2019; Gacíc et al., 2021; Pirro et al., 2022). The SAP can be considered as an oligotrophic environment, where the advection of nutrient are modulated by water mass transport triggered by the BiOS mechanism (Gacíc et al., 2002). The SAP has a very short renewal time compared to other areas, due to the combined effect of deep convection and inflow of oxygen-rich NAdDW together with the inflow of water masses through

the Strait of Otranto (Vilibić and Orlić, 2002). The large amount of water exchanged between the different sub-basins (see Fig. 2 e and f) makes the contribution of biological activity smaller compared to the physical export of oxygen. Mavropoulou et al. (2020) pointed out that the variability of dissolved oxygen was primarily influenced by dynamic processes such as dense water formation, circulation changes, or transients. Šantić et al. (2019) also observed that the biological community in SAP is strongly influenced by mixing and water mass movements.

4.1. Surface layer

In the SAP surface layer, the variability of dissolved oxygen was mainly related to annual primary production (Fig. 3a) and convection events (Fig. 2d), consistent with Hayward (1994) and Gacíc et al. (2002). In spring (i.e., March–June) and summer (i.e., July–September), SOM was observed in the photic zone between 25 m and 70 m depth (in agreement with, e.g., Manca et al., 2004 and Di Biagio et al., 2022), whereas mixing homogenized oxygen distribution in the water column in late autumn and winter (Fig. 3b and c). The high oxygen concentration observed in the SOM was the result of biological activity during the winter/spring period (i.e., the spring bloom), which was trapped by increased summer stratification. The highest levels occurred between 2017 and 2019, coinciding with the highest chlorophyll concentrations (Fig. 3a).

The increase in chlorophyll-*a* and the resulting oxygen production are the result of mixing (MLD in Fig. 2d), making available the nutrients present in the deep layers (Lévy et al., 1998), and the biogeochemical properties of the water masses advected by the NIG circulation (Fig. 4). Indeed, anticyclonic circulation led to an upwelling of the nitracline along the boundaries of the NIG and to an increase in the nutrient content of the water flowing into the Adriatic Sea through the Strait of Otranto (Civitarese et al., 2010).

During convection periods, oxygen produced in the surface layer in the previous spring bloom and oxygen exchanged with atmosphere at the time was mixed along the water column (Fig. 3), benefiting the deep ecosystem and affecting the deep layers of the central and eastern Mediterranean (Manca et al., 2006).

4.2. Oxygen minimum layer (OML)

The intermediate layer of the SAP was characterized by the OML associated with the high salinity water of Levantine origin (i.e. LIW, Zavatarelli et al., 1998, Manca et al., 2006). During convection events, the OML disappeared due to vertical mixing. In 2014, the OML ($\sim 200 \mu\text{mol kg}^{-1}$) was associated with the LIW and ranged from 200 m to 400 m depth (Kokkini et al., 2019; Zavatarelli et al., 1998; Manca et al., 2004). In 2015 and 2016, the combination of weak convection events resulting in reduced vertical advection of dissolved oxygen toward the bottom. The intrusion of lighter and more oxygenated water masses (i.e., NAdDW; Kokkini et al., 2019, Fig. 2b) resulted in a sinking of the LIW core and consequently a deepening of the OML, to 600 m depth (Kokkini et al., 2019; Mihanović et al., 2021). This pattern, described by Kokkini et al. (2019) as double salinity maxima in the water column, also resulted in an oxygen pattern (Fig. 3) showing oxygen maxima vertical offset with respect to salinity maxima.

The strong convection in 2017 drastically changed the structure of the water column (Kokkini et al., 2019), and MLD reached 800 m leading the OML deeper, down to 800 m. OML vanished in late spring

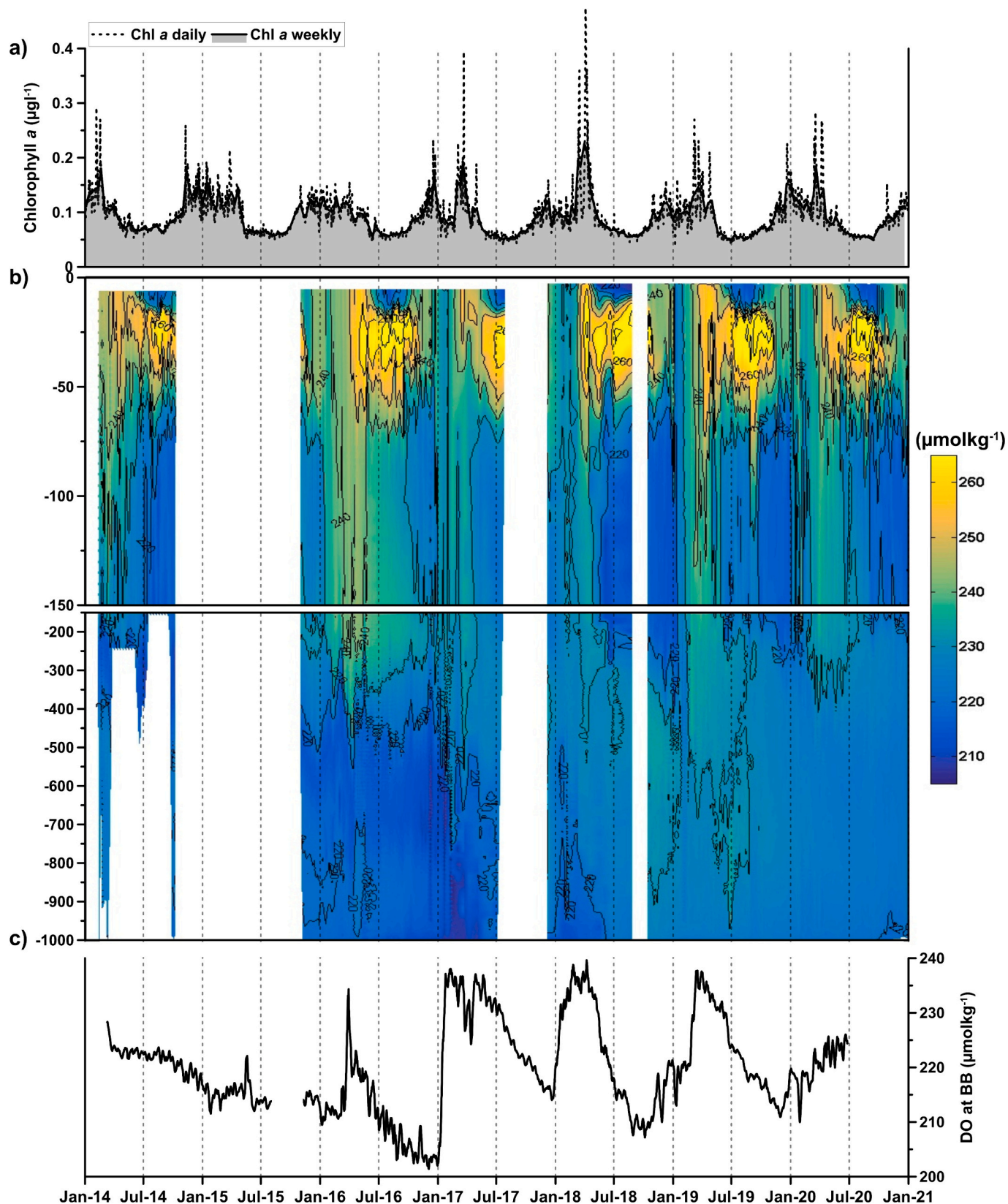


Fig. 3. Surface chlorophyll-a time series (a) as a proxy of primary production, with daily values delimited by the dashed line and weekly field indicated by the filled area. Dissolved oxygen time series (b) split in two panels: 0 m - 150 m on top and 150 m - 1000 m below ($\mu\text{mol kg}^{-1}$). Time series of daily averaged dissolved oxygen (c) at BB site at 590 m depth.

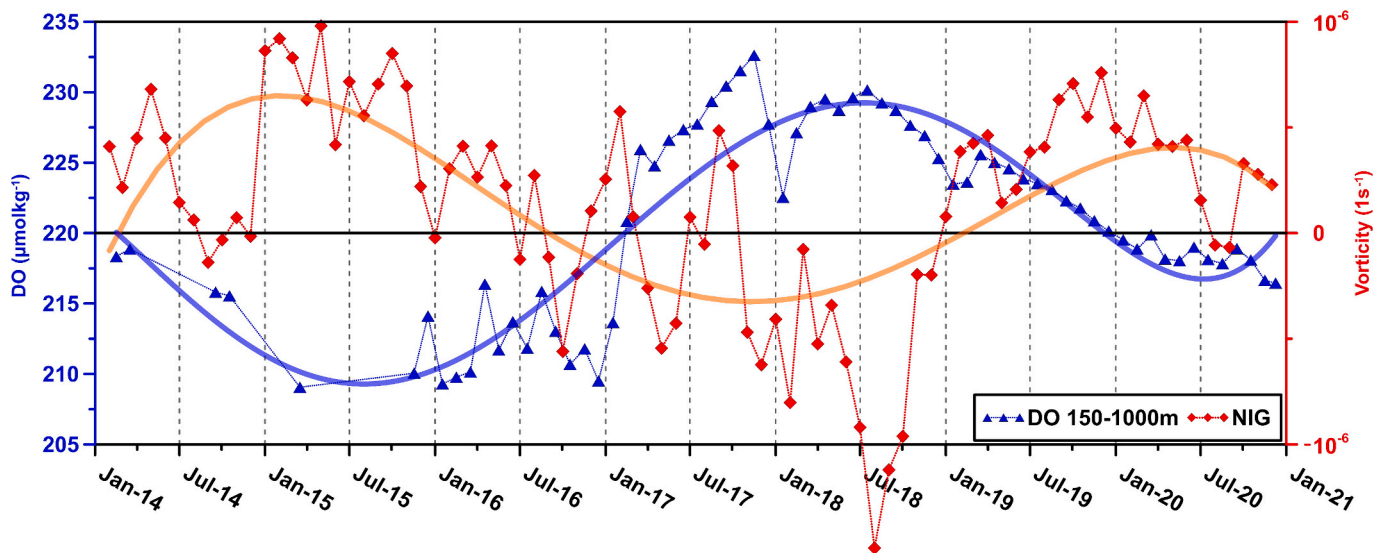


Fig. 4. Time series of the spatially averaged vorticity (red diamonds and dashed line) computed in the northern Ionian Sea (37° – 39° N; 17° – 19.5° E), and monthly dissolved oxygen in the SAP (blue triangles and dashed line) averaged between 150 and 1000 m, from all in situ dataset (i.e. Argo float, ocean glider and p-1200). Data are fitted by polynomial curves, 4th order for vorticity (orange) and 5th order for dissolved oxygen (blue). (For interpretation of the references to colour in this figure legend, the reader is referred to the web version of this article.)

concurrently with the inflow of NAdDW (decrease in temperature and salinity in Fig. 2c and increase in potential density anomaly and dissolved oxygen in Fig. 2d and 3c).

OML became shallower (100–350 m) in 2018, 2019, and 2020 ($\sim 208 \mu\text{mol kg}^{-1}$) and was associated with water masses with salinity and temperature >39 and 14.5°C respectively (Mauri et al., 2021; Menna et al., 2019; Menna et al., 2022a, 2022b). Considering the thermohaline properties of this water mass, it could be described as CIW, which has higher temperature, salinity, and oxygen values compared to the LIW (Manca et al., 2003, 2006). The inflow of this salty and warm water is associated with the northward coastal current along the eastern Ionian Sea, which, unlike the other anticyclonic NIG periods, did not reverse its flow according to the NIG but continued to flow northward (Menna et al., 2019, Menna et al., 2022a, 2022b, Mihanović et al., 2021).

The temporal evolution of the OML could also be related to biological consumption, as a maximum of zooplankton abundance in the subsurface layer was observed in 2018 in SAP (Mauri et al., 2021) and the same period was also characterized by increased phytoplankton biomass (Fig. 3a). This condition leads to a decrease in oxygen concentrations after the dense water formation process (i.e., oxygen-rich surface water mixing with oxygen-poor water), negatively affecting the deep oxygenation of the eastern Mediterranean.

4.3. Deep layer

In the deep layers of SAP, dissolved oxygen is primarily influenced by physical processes (vertical mixing and inflow of water from adjacent sub-basins), as for the eastern Mediterranean Sea (Mavropoulou et al., 2020) and secondary biological activity (Šantić et al., 2019). As shown in Querin et al., 2016, the dynamics in the SAP are characterized by two alternating phases (increase and relaxation) forced by deep convection events and the inflow of cold and newly formed water from the northern Adriatic Sea (i.e., NAdDW), resulting in periods of low and high oxygen concentrations.

The high oxygen concentrations observed from 2017 are closely related to the exceptional air-sea interaction (Kokkini et al., 2019, Mihanović et al., 2021) and to the mixing with the oxygenated intermediate layer. In 2017, deep convection (MLD reached 800 m; Fig. 2d) destroyed the previous oxygen pattern (Fig. 3b and c). The oxygenated

ADW spreads rapidly out of the SAP (Fig. 2e and oxygen reduction after winter mixing in Fig. 3c). Thus, the increased oxygen content observed after the 2017 convection period (Fig. 2c) was due to the ingression of the oxygenated NAdDW (potential density $> 29.2 \text{ kg m}^{-3}$ in Fig. 2d and dissolved oxygen $> \sim 230 \mu\text{mol kg}^{-1}$ in Fig. 3d). Also, the increased oxygen content detected in February 2014 in the deep layers of the SAP (300–1000 m) could be the result of the exceptional convection of 2012 and 2013 (Gačić et al., 2014; Mauri et al., 2016; Querin et al., 2016; Kokkini et al., 2019; Mihanović et al., 2021), similar to 2019 (Fig. 3c).

4.4. Multiannual dissolved oxygen variability

Fig. 4 shows that the time series of NIG vorticity in intermediate and deep layers is out of phase with respect to oxygen concentration in the southern Adriatic Sea, indicating oxygen increase/decrease during anticyclonic/cyclonic phases.

The relationship between the NIG phases and the oxygen concentration in the southern Adriatic was also assessed by Di Biagio et al. (2023), who found a moderate correlation between these variables in the fourth EOF mode of variability. Our results agree with those of Mavropoulou et al. (2020), who observed higher oxygen levels in 1990–1996 ($\sim 205 \mu\text{mol kg}^{-1}$) than in 1996–2010 ($\sim 195 \mu\text{mol kg}^{-1}$), corresponding to the anticyclonic and cyclonic phases of NIG, respectively (Menna et al., 2022a, 2022b); however, it should be noted that the number of observations during this period is very fragmented.

The increase and decrease of dissolved oxygen could be explained by the fact that the anticyclonic NIG (2012–2014 and 2017–2019; Fig. 4) causes a reduced inflow of the less oxygenated LIW, while the cyclonic NIG favours the inflow of LIW (e.g., cyclonic phase of NIG), resulting in a mixing between Levantine and Adriatic waters, which in turn causes a decrease in oxygen content (between 2014 and 2016 and in 2020). The relationship between NIG and oxygen concentration described here differs from that described in previous work (e.g., Vilibic et al., 2002, Manca et al., 2003, 2006), as the OML in the northern Ionian Sea has no effect on oxygen concentration in the southern Adriatic Sea. Prior to our observations, anticyclonic NIG phases were associated with a shallow OML in the northern Ionian Sea (Manca et al., 2003, 2006), leading to the inflow of less oxygenated water toward the SAP. In addition, in a recent modelling work, Liu et al., 2022 estimated the circulation of the NIG and showed that NIG was cyclonic during 1960–1980, which is

consistent with the highest values ($\sim 225 \mu\text{mol kg}^{-1}$) observed by [Mavropoulou et al. \(2020\)](#) and [Vilibić and Orlić \(2002\)](#) in the southern Adriatic Sea.

Similar dissolved oxygen values were also observed between 2017 and 2019 during the anticyclonic NIG phase, suggesting that the relationship between the Ionian Sea and the Adriatic Sea has changed in recent years and the influence of water from the Greek west coast has increased ([Reale et al., 2017](#), [Mihanović et al., 2021](#), [Menna et al., 2022a, 2022b](#)), which also leads to a change in the decadal variation of salinity in the Adriatic Sea ([Gačić et al., 2011](#), [Mihanović et al., 2021](#), [Menna et al., 2021](#), [Menna et al., 2022a, 2022b](#)). Therefore, the inflow of the deep oxygen minimum (e.g. TMW) is not observed during the last anticyclonic periods.

5. Conclusion

In this study, a long-term time series of dissolved oxygen concentrations in the southern Adriatic Sea was analysed integrating different observing systems, in order to increase the understanding of the ventilations dynamic in the deep convection cell of the southern Adriatic Sea and its relationship with the eastern Mediterranean Sea. In general, the southern Adriatic Sea is well oxygenated and we do not detect a deoxygenation trend as for the global ocean, rather we observe a cyclic signal characterized by minimum and maximum oxygen concentrations driven by the advection from adjacent sub-basin.

The SAP is a source of oxygenated water for the deep eastern Mediterranean basin with a short renewal time, so the increase or decrease of oxygen content mainly affects the ecosystems of the deep eastern basin. We analysed the oxygen variability in the southern Adriatic Sea depending on both local and external factors triggered by convection events (driven by severe winters), annual primary production, advection of water from the northern Adriatic Sea (oxygen-rich, cold and fresher, and following the saw-tooth modulation scheme) and the Ionian Sea through the NIG circulation Bimodal Oscillating System. We assume that the very short renewal due to the combined effect of deep convection and inflow of oxygen-rich North Adriatic dense water, together with the inflow of water masses through the Strait of Otranto and the large volume of water exchanged between the different sub-basins, makes the contribution of biological activity smaller compared to the physical export of oxygen.

In recent years, oxygen maxima occurred during the anticyclonic phase of the NIG, while oxygen minima occurred during the cyclonic phase. Dissolved oxygen dynamics are very different from previously observed, suggesting that the process of oxygen enrichment and depletion has changed drastically in recent years. Considering the inflow of very salty and warm water into the intermediate layers of the Adriatic Sea observed since 2018, this may drastically affect deep water formation processes and change the deep advection of dense Adriatic water into the eastern Mediterranean Sea.

Open questions related to the identification of the drivers of the observed changes need to be addressed in future studies. The rotation of NIG is affected by complex interactions with deep water formation in the Adriatic and Aegean Sea that are mutually influenced by large-scale atmospheric circulation, making this issue fundamental to the climate change scenario. Nevertheless, further studies should be conducted to quantify the relative effects of physical transport and biological productivity.

CRedit authorship contribution statement

R. Martellucci: Writing – original draft, Visualization, Validation, Software, Methodology, Investigation, Formal analysis, Data curation, Conceptualization. **M. Menna:** Writing – review & editing, Writing – original draft, Supervision, Investigation. **E. Mauri:** Writing – review & editing, Supervision, Resources, Project administration, Funding acquisition, Conceptualization. **A. Pirro:** Writing – review & editing,

Supervision. **R. Gerin:** Writing – review & editing, Validation, Formal analysis, Data curation, Conceptualization. **F. Paladini de Mendoza:** Writing – review & editing, Methodology, Investigation, Formal analysis, Data curation. **R. Garić:** Writing – review & editing, Methodology, Investigation, Conceptualization. **M. Batistić:** Writing – review & editing, Project administration, Funding acquisition. **V. di Biagio:** Writing – review & editing, Supervision. **P. Giordano:** Writing – review & editing, Supervision, Project administration, Funding acquisition. **L. Langone:** Writing – review & editing, Supervision, Project administration, Funding acquisition. **S. Misericocchi:** Writing – review & editing, Supervision, Project administration, Funding acquisition. **A. Gallo:** Software, Methodology, Data curation. **G. Notarstefano:** Writing – review & editing, Supervision, Funding acquisition. **G. Savonitto:** Formal analysis, Methodology. **A. Bussani:** Software, Data curation. **M. Pacciaroni:** Software, Methodology, Data curation. **P. Zuppelli:** Methodology, Data curation. **P.-M. Poulain:** Writing – review & editing, Supervision, Resources, Project administration, Funding acquisition.

Declaration of competing interest

The authors declare that they have no known competing financial interests or personal relationships that could have appeared to influence the work reported in this paper.

Data availability

all data used in this paper are already available

Acknowledgement

This work is dedicated with affection to Bruno Manca, a colleague and teacher who wrote the history of Easter Mediterranean oceanography, which is mentioned several times in the text, and who recently passed away. We would like to thank Miroslav Gačić, Gianpiero Cossarini, Giorgio dall’Olmo and Giuseppe Civitarese for the useful suggestion and constructive comments during the manuscript preparation. Dr. Vanessa Cardin for providing the E2-M3A data; and Giuseppe Siena for helping with the E2-M3A data collection.

The authors would like to thank the Italian Ministry of Education, University and Research as part of the Argo-Italy program and by the European Commissions, as part of the Copernicus CMEMS-TAC programs and the Croatian Science Foundation (AdMedPlan, IP-2014-09-2945; DiVMAD, IP-2019-04-9043).

The maintenance of BB and FF fixed moorings over time was only possible thanks to the support of the following projects: European Community’s Seventh Framework Programme projects HERMIONE (Grant agreement No. 226354) and COCONET (Grant agreement No.287844) of the European Commission, the Flagship project RIT-MARE SP5_WP3_AZ1 (the Italian Research for the Sea). This work was supported also by the EMSO-Italia Joint Research Unit (JRU). The authors thank the cruise participants who helped with the mooring servicing, in particular the captain and the crew members of the R/V’s Urania, Minerva Uno, G. Dallaporta, Laura Bassi and OGS Explora, and of the fishing boats Pasquale & Cristina, and Attila.

Appendix A. Supplementary data

Supplementary data to this article can be found online at <https://doi.org/10.1016/j.jmarsys.2024.103988>.

References

- Artegiani, A., Bregant, D., Paschini, E., Pinardi, N., Raicich, F., Russo, A., 1997. The Adriatic Sea general circulation. Part I. Air–sea interactions and water mass structure. *J. Phy. Oceanogr.* 27, 1492–1514.
- Batistić, M., Viličić, D., Kovačević, V., Jasprica, N., Garić, R., Lavigne, H., Carić, M., 2019. Occurrence of winter phytoplankton bloom in the open southern Adriatic:

- relationship with hydroclimatic events in the eastern Mediterranean. *Cont. Shelf Res.* 174, 12–25.
- Bensi, M., Cardin, V., Rubino, A., Notarstefano, G., Poulain, P.M., 2013. Effects of winter convection on the deep layer of the Southern Adriatic Sea in 2012. *J. Geophys. Res. Ocean* 118, 6064–6075. <https://doi.org/10.1002/2013JC009432>.
- Bignami, F., Salusti, E., Schiarini, S., 1990. Observation on a bottom vein of dense water in the southern Adriatic and Ionian seas. *J. Geophys. Res.* 95, 7249–7259.
- Bittig, H.C., Körtzinger, A., Neill, C., Van Ooijen, E., Plant, J.N., Hahn, J., et al., 2018. Oxygen optode sensors: principle, characterization, calibration, and application in the ocean. *Front. Mar. Sci.* 4, 429.
- Breitburg, D., Levin, L.A., Oschlies, A., Grégoire, M., Chavez, F.P., Conley, D.J., et al., 2018. Declining oxygen in the global ocean and coastal waters. *Science* 359 (6371).
- Cabanes, C., Thierry, V., Lagadec, C., 2016. Improvement of bias detection in Argo float conductivity sensors and its application in the North Atlantic. *Deep Sea Res. Part I: Oceanogr. Res. Pap.* 114, 128–136. <https://doi.org/10.1016/j.dsr.2016.05.007>.
- Cabanes, C., Angel-Benavides, I., Buck, J., Coatanoan, C., Dobler, D., Herbert, G., Klein, B., Maze, G., Notarstefano, G., Owens, B., 2021. DMQC Cookbook for Core Argo Parameters. <https://doi.org/10.13155/78994>.
- Cardin, V., Wirth, A., Khosravi, M., Gacic, M., 2020. South Adriatic 'recipes': estimating the vertical mixing in the deep pit. *Front. Mar. Sci.* 7, 565982 <https://doi.org/10.3389/fmars.2020.565982>.
- Carpenter, J.H., 1965. The accuracy of the Winkler method for dissolved oxygen analysis. *Limnol. Oceanogr.* 10 (1), 135–140. <https://doi.org/10.4319/lo.1965.10.1.0135>.
- Chiggiato, J., Bergamasco, A., Borghini, M., Falcieri, F.M., Falco, P., Langone, L., Miserocchi, S., Russo, A., Schroeder, K., 2016. Dense-water bottom currents in the Southern Adriatic Sea in spring 2012. *Mar. Geol.* 375, 134–145. <https://doi.org/10.1016/j.margeo.2015.09.005>.
- Civitaresse, G., Gačić, M., Lipizer, M., Eusebi Borzelli, G.L., 2010. On the impact of the bimodal oscillating system (BIOS) on the biogeochemistry and biology of the Adriatic and Ionian seas (eastern Mediterranean). *Biogeosciences* 7, 3987–3997. <https://doi.org/10.5194/bg-7-3987-2010>.
- Civitaresse, G., Gačić, M., Batistić, M., Bensi, M., Cardin, V., Dulčić, J., Menna, M., 2023. The BIOS mechanism: history, theory, implications. *Prog. Oceanogr.* 103056.
- Coppola, L., Legendre, L., Lefevre, D., Prieur, L., Taillandier, V. and Diamond Riquier E., 2018. Seasonal and inter-annual variations of dissolved oxygen in the northwestern Mediterranean Sea (DYFAMED site). *Prog. Oceanogr.* 162 187–201, doi:<https://doi.org/10.1016/j.pocean.2018.03.001>, 2018.
- de Boyer Montégut, C., Madec, G., Fischer, A.S., Lazar, A., Iudicone, D., 2004. Mixed layer depth over the global ocean: an examination of profile data and a profile-based climatology. *J. Geophys. Res.* 109, C12003. <https://doi.org/10.1029/2004JC002378>.
- De Santis, A., Chiappini, M., Marinaro, G., Guardato, S., Conversano, F., D'Anna, G., Di Mauro, D., Cardin, V., Carluccio, R., Rende, S.F., Giordano, R., Rossi, L., Simeone, F., Giacomozzi, E., Fertitta, G., Costanza, A., Donnarumma, G.P., Riccio, R., Siena, G., Civitaresse, G., 2022. InSEA project: initiatives in supporting the consolidation and enhancement of the EMSO infrastructure and related activities. *Front. Mar. Sci.* 9, 846701 <https://doi.org/10.3389/fmars.2022.846701>.
- Di Biagio, V., Salon, S., Feudale, L., Cossarini, G., 2022. Subsurface oxygen maximum in oligotrophic marine ecosystems: mapping the interaction between physical and biogeochemical processes. *Biogeosciences* 19, 23. <https://doi.org/10.5194/bg-19-5553-2022>.
- Di Biagio, V., Riccardo, Martellucci R., Menna, M., Teruzzi, A., Amadio, C., Mauri, E., Cossarini, G., 2023. Dissolved oxygen as indicator of multiple drivers of the marine ecosystem: the southern Adriatic Sea case study. In: 7th edition of the Copernicus Marine Service Ocean State Report (OSR 7), State of the Planet. (accepted).
- Escudier, R., Clementi, E., Cipollone, A., Pistoia, J., Drudi, M., Grandi, A., Lyubartsev, V., Lecci, R., Aydogdu, A., Delrosso, D., Omar, M., Masina, S., Coppini, G., Pinardi, N., 2021. A high resolution reanalysis for the Mediterranean Sea. *Front. Earth Sci.* 9 <https://doi.org/10.3389/feart.2021.702285>.
- Falkowski, P.G., Algeo, T., Codispoti, L., Deutsch, C., Emerson, S., Hales, B., et al., 2011. Ocean deoxygenation: past, present, and future. *Eos* 92 (46), 409–410.
- Gačić, M., Civitaresse, G., Miserocchi, S., Cardin, V., Crise, A., Mauri, E., 2002. The open-ocean convection in the Southern Adriatic: a controlling mechanism of the spring phytoplankton bloom. *Cont. Shelf Res.* 1897–1908.
- Gačić, M., Borzelli, G.E., Civitaresse, G., Cardin, V., Yari, S., 2010. Can internal processes sustain reversals of the ocean upper circulation? The Ionian Sea example. *Geophys. Res. Lett.* 37 (9), L09608. <https://doi.org/10.1029/2009JC005749>.
- Gačić, M., Civitaresse, G., Eusebi Borzelli, G.L., Kovačević, V., Poulain, P.M., et al., 2011. On the relationship between the decadal oscillations of the northern Ionian Sea and the salinity distributions in the eastern Mediterranean. *J. Geophys. Res. Oceans* 116, C12. <https://doi.org/10.1029/2011JC007280>.
- Gačić, M., Civitaresse, G., Kovačević, V., Ursella, L., Bensi, M., Menna, M., Cardin, V., Poulain, P.-M., Cosoli, S., Notarstefano, G., Pizzi, C., 2014. Extreme winter 2012 in the Adriatic: an example of climatic effect on the BIOS rhythm. *Ocean Sci.* 10, 513–522. <https://doi.org/10.5194/os-10-513-2014>.
- Gačić, M., Ursella, L., Kovačević, V., Menna, M., Malačić, V., Bensi, M., et al., 2021. Impact of dense-water flow over a sloping bottom on open-sea circulation: laboratory experiments and an Ionian Sea (Mediterranean) example. *Ocean Sci.* 17, 975–996. <https://doi.org/10.5194/os-17-975-2021>.
- Gallo, A., Martellucci, R., 2022. The 2013–2021 Argo float salinity dataset in the Southern Adriatic Pit. DATASET. <https://doi.org/10.13120/BXF7-PB83>.
- Garcia, H.E., Keeling, R.F., 2001. On the global oxygen anomaly and air-sea flux. *J. Geophys. Res.: Oceans* 106 (C12), 31155–31166.
- Gerin, R., Martellucci, R., Notarstefano, G., Mauri, E., 2020a. Float oxygen data calibration with discrete Winkler samples in the South Adriatic Sea. *Rel. 2020/30 Sez. OCE 9 MAOS*.
- Gerin, R., Martellucci, R., Mauri, E., Kokkini, Z., Medeot, N., et al., 2020b. Oxygen concentration in the South Adriatic Sea: the gliders measurements. *Rel. 2020/30 Sez. OCE 9 MAOS*.
- Gilly, W.F., Beman, J.M., Litvin, S.Y., Robison, B.H., 2013. Oceanographic and biological effects of shoaling of the oxygen minimum zone. *Ann. Rev. Mar. Sci.* 5 (1), 393–420.
- Hayward, T.L., 1994. The shallow oxygen maximum layer and primary production. *Deep Sea Res. I: Oceanogr. Res. Pap.* 41 (3), 559–574.
- Houpert, L., Durrieu de Madron, X., Testor, P., Bosse, A., d'Ortenzio, F., Bouin, M.N., et al., 2016. Observations of open-ocean deep convection in the northwestern Mediterranean Sea: Seasonal and interannual variability of mixing and deep water masses for the 2007–2013 Period. *J. Geophys. Res. Oceans* 121 (11), 8139–8171.
- Johnson, K.S., Plant, J.N., Riser, S.C., Gilbert, D., 2015. Air oxygen calibration of oxygen optodes on a profiling float array. *J. Atmos. Oceanic Technol.* 32 (11), 2160–2172.
- Josey, S.A., Somot, S., Tsimplis, M., 2011. Impacts of atmospheric modes of variability on Mediterranean Sea surface heat exchange. *J. Geophys. Res. Oceans* 116 (C2).
- Keeling, R.F., Körtzinger, A., Gruber, N., 2010. Ocean deoxygenation in a warming world. *Ann. Rev. Mar. Sci.* 2 (1), 199–229.
- Kokkini, Z., Mauri, E., Gerin, R., Poulain, P.-M., Simoncelli, S., Notarstefano, G., 2019. On the salinity structure in the south Adriatic as derived from float and glider observations in 2013–2016. *Deep Sea Res. II* 2020, 104625.
- Kovač, Ž., Platt, T., Ninčević, Gladan Ž., Morović, M., Sathyendranath, S., et al., 2018. A 55-year time series station for primary production in the Adriatic Sea: data correction, extraction of photosynthesis parameters and regime shifts. *Remote Sens. (Basel)* 10, 1460.
- Krokos, G., Velaoras, D., Korres, G., Perivoliotis, L., Theocharis, A., 2014. On the continuous functioning of an internal mechanism that drives the eastern Mediterranean thermohaline circulation: the recent activation of the Aegean Sea as a dense water source area. *J. Mar. Sys.* 129, 484–489. <https://doi.org/10.1016/J.JMARSYS.2013.10.002>.
- Lévy, M., Mémerly, L., André, J.M., 1998. Simulation of primary production and export fluxes in the northwestern Mediterranean Sea. *J. Mar. Res.* 56, 197–238.
- Lipizer, M., Partescano, E., Rabitti, A., Giorgetti, A., Crise, A., 2014. Qualified temperature, salinity and dissolved oxygen climatologies in a changing Adriatic Sea. *Ocean Sci.* 10, 771–797. <https://doi.org/10.5194/os-10-771-2014>.
- Liu, F., Mikolajewicz, U., Katharina, D.S., 2022. Drivers of the decadal variability of the north Ionian gyre upper layer circulation during 1910–2010: a regional modelling study. *Climate Dynam.* 58 (7–8), 2065–2077.
- Macias, D., Garcia-Goriz, E., Stips, A., 2018. Deep winter convection and phytoplankton dynamics in the NW Mediterranean Sea under present climate and future (horizon 2030) scenarios. *Sci. Rep.* 8, 6626. <https://doi.org/10.1038/s41598-018-24965-0>.
- Malanotte-Rizzoli, P., Eremeev, V.N., 1999. The Eastern Mediterranean as a Laboratory Basin for the Assessment of Contrasting Ecosystems. Springer, Netherlands.
- Malanotte-Rizzoli, P., Manca, B.B., d'Alcala, M.R., Theocharis, A., Souvermezoglou, E., et al., 1997. A synthesis of the Ionian Sea hydrography, circulation and water mass pathways during POEM-Phase I. *Prog. Oceanogr.* 39 (3), 153–204.
- Manca, B.B., Kovacevic, V., Gačić, M., Viezzoli, D., 2002. Dense water formation in the southern Adriatic Sea and spreading into the Ionian Sea in the period 1997–1999. *J. Mar. Sys.* 33–34, 133–154.
- Manca, B.B., Budillon, G., Scarazzato, P., Ursella, L., 2003. Evolution of dynamics in the eastern Mediterranean affecting water mass structures and properties in the Ionian and Adriatic Seas (1995–1999). *J. Geophys. Res. Oceans* 108, C9. <https://doi.org/10.1029/2002JC001664>.
- Manca, B., Burca, M., Giorgetti, A., Coatanoan, C., Garcia, M.J., Iona, A., 2004. Physical and biochemical averaged vertical profiles in the Mediterranean regions: an important tool to trace the climatology of water masses and to validate incoming data from operational oceanography. *J. Mar. Sys.* 48 (1–4), 83–116, 2004.
- Manca, B.B., Ibello, V., Pacciaroni, M., Scarazzato, P., Giorgetti, A., 2006. Ventilation of deep waters in the Adriatic and Ionian Seas following changes in thermohaline circulation of the Eastern Mediterranean. *Climate Res.* 31 (2–3), 239–256.
- Marshall, J., Schott, F., 1999. Open-ocean convection, observations, theory, and models. *Rev. Geophys.* 37, 1–64.
- Martellucci, R., Salon, S., Cossarini, G., Piermattei, V., Marcelli, M., 2021. Coastal phytoplankton bloom dynamics in the Tyrrhenian Sea: advantage of integrating in situ observations, large-scale analysis and forecast systems. *J. Mar. Sys.* 218, 103528.
- Matear, R.J., Hirst, A.C., McNeil, B.I., 2000. Changes in dissolved oxygen in the Southern Ocean with climate change. *Geochem. Geophys. Geosyst.* 1, 1050. <https://doi.org/10.1029/2000GC000086>.
- Mauri, E., Gerin, R., Poulain, P.-M., 2016. Measurements of water-mass properties with a glider in the South-Western Adriatic Sea. *J. Oper. Oceanogr.* 9, s3–s9. <https://doi.org/10.1080/1755876X.2015.1117766>.
- Mauri, E., Menna, M., Garić, R., Batistić, M., Libralato, S., et al., 2021. Recent changes of the salinity distribution and zooplankton community in the south Adriatic pit. Copernicus marine service ocean state report. *J. Oper. Oceanogr.* 14, 102–109. <https://doi.org/10.1080/1755876X.2021.1946240>.
- Mavropoulou, A.M., Vervatis, V., Sofianos, S., 2020. Dissolved oxygen variability in the Mediterranean Sea. *J. Mar. Sys.* 208, 103348.
- Menna, M., Reyes-Suarez, N.C., Civitaresse, G., Gačić, M., Poulain, P.-M., Rubino, A., 2019. Decadal variations of circulation in the Central Mediterranean and its interactions with the mesoscale gyres. *Deep Sea Res. II* 2019 (164), 14–24. <https://doi.org/10.1016/j.dsr2.2019.02.004>.
- Menna, M., Gačić, M., Martellucci, R., Notarstefano, G., Fedele, G., et al., 2022a. Climatic, decadal and interannual variability in the upper layer of the Mediterranean

- Sea using remotely sensed and in-situ data. *Remote Sens. (Basel)* 2022 (14), 1322. <https://doi.org/10.3390/rs14061322>.
- Menna, M., Martellucci, R., Notarstefano, G., Mauri, E., Gerin, R., et al., 2022b. Record-breaking high salinity in the South Adriatic Pit in 2020, copernicus marine service ocean state report 6. *J. Oper. Oceanogr.* 15, 199–205.
- Mihanovic, H., Vilibic, I., Carniel, S., Tudor, M., Russo, A., et al., 2013. Exceptional dense water formation on the Adriatic shelf in the winter of 2013. *Ocean Sci.* 9, 561–572.
- Mihanović, H., Vilibić, I., Šepić, J., Matić, F., Ljubešić, Z., et al., 2021. Observation, preconditioning and recurrence of exceptionally high salinities in the Adriatic Sea. *Front. Mar. Sci.* 8, 834. <https://doi.org/10.3389/fmars.2021.672210>.
- Misrocchi, S., Paladini de Mendoza, F., Verazzo, G., 2023. Southern Adriatic BB and FF mooring data management plan for EMSO-ERIC. Zenodo. <https://doi.org/10.5281/zenodo.10412751>.
- Notarstefano, G., Menna, M., Legeais, J.F., 2019. Reversal of the Northern Ionian circulation in 2017. *J. Oper. Oceanogr.* 12, S108, in von Schuckmann et al., 2019. <https://doi.org/10.1080/1755876X.2019.1633075>.
- Oschlies, A., Brandt, P., Stramma, L., Schmidtko, S., 2018. Drivers and mechanisms of ocean deoxygenation. *Nat. Geosci.* 11 (7), 467–473.
- Owens, W.B., Wong, A.P.S., 2009. An improved calibration method for the drift of the conductivity sensor on autonomous CTD profiling floats by θ -S climatology. *Deep Sea Res. I: Oceanogr. Res. Pap.* 56 (3), 450–457. <https://doi.org/10.1016/j.dsr.2008.09.008>.
- Paladini de Mendoza, F., Schroeder, K., Langone, L., Chiggiato, J., Borghini, M., Giordano, P., Verazzo, G., Misrocchi, S., 2022. Deep-water hydrodynamic observations of two moorings sites on the continental slope of the southern Adriatic Sea (Mediterranean Sea). *Earth System Science Data* 14 (12), 5617–5635.
- Paladini de Mendoza, F., Schroeder, K., Misrocchi, S., Borghini, M., et al., 2023. Sediment resuspension and transport processes during dense water cascading events along the continental margin of the southern Adriatic Sea (Mediterranean Sea). *Mar. Geo.* 107030.
- Pierce, S.D., Barth, J.A., Shearman, R.K., Erofeev, A.Y., 2012. Declining oxygen in the Northeast Pacific. *J. Phy. Oceanogr.* 42 (3), 495–501.
- Pirro, A., Mauri, E., Gerin, R., Martellucci, R., Zuppelli, P., Poulain, P.M., 2022. New insights on the formation and breaking mechanism of convective cyclonic cones in the South Adriatic Pit during winter 2018. *J. Phy. Oceanogr.* 52 (9), 2049–2068.
- Pranić, P., Denamiel, C., Vilibić, I., 2021. Performance of the Adriatic Sea and coast (AdriSC) climate component – a COAWST V3.3-based one-way coupled atmosphere–ocean modelling suite: ocean results. *Geosci. Model Dev.* 14, 5927–5955. <https://doi.org/10.5194/gmd-14-5927-2021>.
- Querini, S., Cossarini, G., Solidoro, C., 2013. Simulating the formation and fate of dense water in a midlatitude marginal sea during normal and warm winter conditions. *J. Geophys. Res. Oceans* 118, 885–900.
- Querini, S., Bensi, M., Cardin, V., Solidoro, C., Bacer, S., et al., 2016. Saw-tooth modulation of the deep-water thermohaline properties in the southern Adriatic Sea. *J. Geophys. Res. Oceans* 121 (4585–4600), 2016. <https://doi.org/10.1002/2015JC011522>.
- Reale, M., Salon, S., Crise, A., Farneti, R., Mosetti, R., Sannino, G., 2017. Unexpected covariant behavior of the Aegean and Ionian seas in the period 1987–2008 by means of a nondimensional sea surface height index. *J. Geophys. Res. Oceans* 122 (10), 8020–8033.
- Reale, M., Salon, S., Somot, S., Solidoro, C., Giorgi, F., Crise, A., Cossarini, G., Lazzari, P., Sevault, F., 2020. Influence of large-scale atmospheric circulation patterns on nutrient dynamics in the Mediterranean Sea in the extended winter season (October–March) 1961–1999. *Climate Res.* 52, 117–136.
- Reale, M., Cossarini, G., Lazzari, P., Lovato, T., Bolzon, G., Masina, S., Salon, S., 2021. Acidification, deoxygenation, nutrient and biomasses decline in a warming Mediterranean Sea. *Biogeosci.* 19 (17), 4035–4065. <https://doi.org/10.5194/bg-19-4035-2022>.
- Rio, M.H., Pascual, A., Poulain, P.M., Menna, M., Barceló, B., Tintoré, J., 2014. Computation of a new mean dynamic topography for the Mediterranean Sea from model outputs, altimeter measurements and oceanographic in situ data. *Ocean Sci.* 10, 731–744. <https://doi.org/10.5194/os-10-731-2014>.
- Šantić, D., Kovačević, V., Bensi, M., Giani, M., Vrdoljak, A., Ordulj, M., et al., 2019. Picoplankton distribution and activity in the deep waters of the southern Adriatic Sea. *Water* 11, 1655.
- Schmidtko, S., Stramma, L., Visbeck, M., 2017. Decline in global oceanic oxygen content during the past five decades. *Nature* 542 (7641), 335–339.
- Schott, F., Send, U., Fischer, J., Stramma, L., Desaubies, Y., 1996. Observations of deep convection in the Gulf of Lions, northern Mediterranean, during the winter of 1991/92. *J. Phys. Oceanogr.* 26, 505–524. [https://doi.org/10.1175/1520-0485\(1996\)026<0505:OODCIT.2.0.CO;2](https://doi.org/10.1175/1520-0485(1996)026<0505:OODCIT.2.0.CO;2).
- Shulenberg, E., Reid, J.L., 1981. The Pacific shallow oxygen maximum, deep chlorophyll maximum, and primary productivity, reconsidered. *Deep Sea Res. I* 28 (9), 901–919.
- Souvermezoglou, E., Krasakopoulou, E., Pavlidou, A., 1999. Temporal variability in oxygen and nutrient concentrations in the southern Aegean Sea and the straits of the Cretan arc. *Prog. Oceanogr.* 44 (4), 573–600.
- Stramma, L., Schmidtko, S., Levin, L.A., Johnson, G.C., 2010. Ocean oxygen minima expansions and their biological impacts. *Deep Sea Res. I* 57 (4), 587–595.
- Takeshita, Y., Martz, T.R., Johnson, K.S., Plant, J.N., Gilbert, D., Riser, S.C., et al., 2013. A climatology-based quality control procedure for profiling float oxygen data. *J. Geophys. Res. Oceans* 118 (10), 5640–5650.
- Testor, P., Bosse, A., Houpert, L., Margirier, F., Mortier, L., Legoff, H., et al., 2018. Multiscale observations of deep convection in the northwestern Mediterranean Sea during winter 2012–2013 using multiple platforms. *J. Geophys. Res. Oceans* 123 (3), 1745–1776.
- Thierry, V., Bittig, H., Gilbert, D., Kobayashi, T., Kanako, S., Schmid, C., 2022. 656 Processing Argo oxygen data at the DAC level. Version 2.3.3, April 27th, 2022. In: Villefranche-sur-mer, 657. Mer:IFREMER for Argo BGC Group. <https://doi.org/10.13155/39795>.
- Ulses, C., Estournel, C., Fourrier, M., Coppola, L., Kessouri, F., et al., 2021. Oxygen budget of the northwestern Mediterranean deep-convection region. *Biogeosci.* 18, 937–960. <https://doi.org/10.5194/bg-18-937-2021>.
- Vilibić, I., Orlić, M., 2002. 2002 Adriatic water masses, their rates of formation and transport through the Otranto Strait. *Deep Sea Res. Part I* (49), 1321–1340.
- Volpe, G., Colella, S., Brando, V.E., Forneris, V., La Padula, F., Di Cicco, A., Santoleri, R., 2019. Mediterranean ocean colour Level 3 operational multi-sensor processing. *Ocean Sci.* 15 (1), 127–146.
- Wong, A.P.S., Johnson, G.C., Owens, W.B., 2003. Delayed-mode calibration of autonomous CTD profiling float salinity data by theta-S climatology. *J. Atmos. Oceanic Tech.* 20, 308–318. [https://doi.org/10.1175/1520-0426\(2003\)020<0308:DMCOAC>2.0.CO;2](https://doi.org/10.1175/1520-0426(2003)020<0308:DMCOAC>2.0.CO;2).
- Wong, A.P.S., Wijffels, S.E., Riser, S.C., Poulouien, S., Hosoda, S., Roemmich, D., Gilson, J., Johnson, G.C., Martini, K., Murphy, D.J., et al., 2020. Argo data 1999–2019: two million temperature-salinity profiles and subsurface velocity observations from a global array of profiling floats. *Front. Mar. Sci.* 7, 700. <https://doi.org/10.3389/fmars.2020.00700>.
- Yari, S., Kovačević, V., Cardin, V., Gačić, M., Bryden, H.L., 2012. Direct estimate of water, heat, and salt transport through the Strait of Otranto. *J. Geophys. Res. Oceans* 117, C9.
- Zavatarelli, M., Raicich, F., Bregant, D., Russo, A., Artegiani, A., 1998. Climatological biogeochemical characteristics of the Adriatic Sea. *J. Mar. Syst.* 18, 227–263.